

**Response to comments on “PMIF v1.0: an inversion system to estimate the potential of satellite observations to monitor fossil fuel CO<sub>2</sub> emissions” by Y. Wang et al.**

We thank the referee for reviewing our manuscript. Please find attached a point-by point reply (in black) to each of the comments raised by the referee (in blue) with legible text and figures organized along the text. For your convenience, changes in the revised manuscript are highlighted with dark red. All the pages and line numbers correspond to the original version of text.

This study assesses the potential of satellite imagery of a future mission CO<sub>2</sub>M XCO<sub>2</sub> to constrain the emissions from cities and power plants over the whole globe for one year. To reduce the computational cost of the traditionally used 3-D full transport models, this study simplified the observation operator with a few idealized hypotheses: (a) a Gaussian plume model, no model errors, (b) no overlapping effects from nearby hotspots, (c) no impact of natural carbon cycle fluxes. It is useful to get a global-scale estimate for the potential of emission uncertainty reductions for the proposed mission – even though the results are not very positive in terms of CO<sub>2</sub> measurements’ potential in constraining fossil fuel CO<sub>2</sub> emissions alone given those idealized setups.

**Response:**

We would like to clarify the point (b) listed above by the reviewer. Actually, there can be some overlapping between the plumes generated by nearby clumps in the PMIF. In Eulerian transport model, the plumes from nearby sources can converge along atmospheric circulation. However, here, since using a classical Gaussian plume model, the plumes are straight along the wind direction. Therefore, the plumes from two nearby clumps can cross each other, but they’ll systematically diverge on long distances, which, in some cases, can lead to a significant underestimation of the plume overlapping. To make it clearer, we revised the sentences Ln 506-508: “...Firstly, the plumes generated by the Gaussian plume model are straight along the wind direction at the source pixel. As a result, **we allow the plumes from nearby clumps to potentially cross each other, but these plumes will systematically diverge on long distances. The Gaussian plume model cannot reproduce plumes overlapping along the atmospheric circulation like Eulerian transport models. In this sense, the overlapping effect of plumes can be underestimated in PMIF. In a realistic situation of atmospheric transport, if plumes from multiple clumps overlap very often, the inversion performance for individual clumps will be degraded since it will have the difficulties to accurately attribute the XCO<sub>2</sub> signals to individual clumps.**”

**General comments:**

The authors highlight the global scope of this study, but no global distribution is shown. Fig. 6 shows information about US and China, why only these two regions? The global results are aggregated with emission density bins (Fig 2 - 5), which I assume is not the only determining factor. With simple statistics of median spread, a lot of information is lost. It does not really provide a "global" view. Fig. 1 highlighted the impacts of wind speed, which may create spatial patterns that overlay with emission density maps. Such information may reveal a better global overview.

**Response:**

We synthesize the global results with the plot of median values and the spread in Figs. 2-5. Figure 6 is shown to prove that the frequency of clear-sky largely explains the large variations within each emission bin. We agree with the reviewer that the inversion results are mainly driven by a combination of emission rates, wind speed and frequency of clear-sky days. However, plotting clumps' uncertainty on top of clump emissions or wind speed would make the figure too saturated to read. (Figure 6c and d are already close to a saturation of dots). Following the reviewer advice, we have produced figures like Figure 6c and d for all the regions of the globe. However, since they do not bring much more qualitative insights than Figure 6c and d, we have put them in the supplementary material. In the main text, we remind the readers to refer to these figures accordingly:

Ln 410: “At regional scale (Figs. S4, S5), South America, North America, and Africa tend to have larger N20 values for same bin of clump annual emission than the other regions, while Middle East and Asia have the lowest ones. **In addition, there are large variations and spatial heterogeneity in the N20 values within each emission bins (Fig. S5), which will be further discussed in Sect. 4.**”

Ln 545: “... These results illustrate the dependence of the potential of satellite observations to constrain emissions on the frequency of clear-sky conditions. **The relative uncertainty in the inversion of the emissions from a clump is primarily driven by the budget of these emissions, and by the wind speed (as illustrated by Fig. 1). The frequency of clear-sky days modulates the number of direct observation of the plume from a clump and thus the number of days for which the inversion can decrease the uncertainty when ignoring temporal auto-correlations in the prior uncertainty in Exp-NoCor. The frequency of clear-sky day, together with the emission rate and wind speed, are the main drivers of the posterior uncertainty in daily to annual emissions when accounting for temporal auto-correlations in the prior uncertainty.**”

Also, a posterior uncertainty of 20% has been used as a benchmark throughout the paper (given a 30% prior uncertainty). However, only a few cases/days can meet such a requirement. Thus, it may be more helpful to show what posterior uncertainty can be achieved for a given length of days across typical regions (e.g., using a 2-D matrix?)

**Response:**

Firstly, we stress that the prior uncertainties are different at different time scale. In all the experiments, the prior uncertainty is 30% for annual emissions. When decomposing the uncertainty of annual emissions to the scales of 3 h and 21 h time windows, the resulting uncertainties largely depend on the assumption about the temporal auto-correlations (Sect. 2.6). In the ASS scenario, the prior uncertainty for 3 h emissions is  $\sqrt{(44\%^2+26\%^2)}=51\%$ , while in NoCor scenario, it is 614%.

Eq. (1) shows that the posterior uncertainty and uncertainty reduction depend on the prior uncertainty. For example, if the projection of uncertainties in satellite observations on the uncertainty in emissions (i.e.  $\mathbf{M}^T\mathbf{R}^{-1}\mathbf{M}$ ) equals to 50% for a single 3 h time window, in ASS scenario, the posterior uncertainty equals to  $\sqrt{1/(1/(51\%)^2+1/(50\%)^2)}=36\%$ , while in NoCor, the posterior uncertainty equals to 50%. In this situation, if the benchmark is chosen too high (e.g. 50%), it is too easy for ASS scenario, while it still requires a lot of constraints from satellite observations in NoCor scenario. If we choose 60% as the benchmark for assessing the posterior uncertainty, then the prior uncertainty in emissions in ASS will always below the

benchmark, even without conducting the inversion. Given different values of prior uncertainty in different scenarios, it is not easy to find a metric to fairly compare the results from different scenarios. We choose 20% as a benchmark because if the posterior uncertainty is below 20%, it is mainly determined by the projection of uncertainties in satellite observations on the uncertainty of emissions.

Furthermore, the posterior uncertainty in the emissions within 3 h time window or in the daily emissions, and thus the number of N20 and D20 are among the diagnostics we investigated on the potential of satellite observations. We also assessed the posterior uncertainty at annual scale, which integrates the uncertainty in all time windows, not only those whose uncertainty is smaller than 20%.

In the first version of this paper, we did consider to use a 2-D matrix to show the results, as shown in Fig. R2. We think such a 2-D matrix plot has its own disadvantages: 1) as stated above, the posterior uncertainty also depends on the prior uncertainty, if the threshold is chosen high, it does not properly represent the actual constraints from satellite observations; 2) such a plot cannot show the large variations in the number of cases within each emission bin. But this information is easy to read from the whisker plot in Fig. 3-5; and 3) such a 2-D matrix plot cannot compare the performance of the inversion in different experiments directly. Given the close values of some experiments (e.g. AMS and ASS in Fig. 3), the difference between experiments cannot be noticed by eye from separate 2-D matrix plots. Given these considerations, we decided to use the plots that have been shown in the paper, which can synthesize as the most information as we want to deliver, and also makes it possible to compare the performance for different experiments.

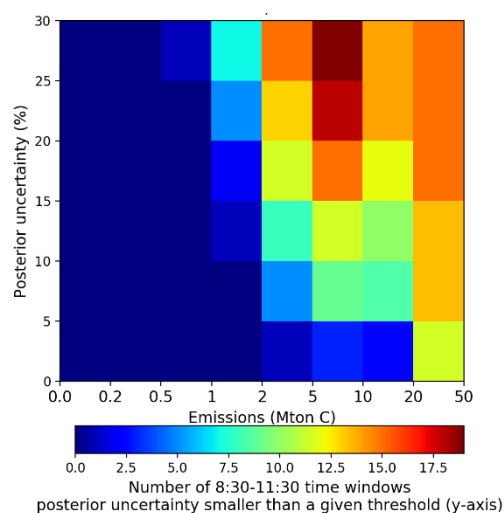


**Figure R2** Number of 8:30-11:30 time windows (color) within a year for which the 3 h emissions are constrained with a posterior uncertainty less than a given threshold (y-axis) in the Exp-NoCor experiment.

In the revised manuscript, we add in Fig. 2 the 2-D matrix plot to illustrate the number of cases under different threshold. But we do not do that for the other diagnostics. And we add some discussions about this figure:

“At regional scale (Fig. S4), South America, North America, and Africa tend to have larger N20 values for same bin of clump annual emission than the other regions, while Middle East and Asia have the lowest ones. **In addition, there are large variations and spatial**

heterogeneity in the N20 values within each emission bins (Fig. S5), which will be further discussed in Sect. 4.

We also show the numbers of 8:30-11:30 time windows per clump being labeled as “well-constrained” when the posterior uncertainty of 3 h mean emission is smaller than other thresholds, e.g. 10% and 30% (Fig. 2b). In general, using a posterior uncertainty larger than 20% as a threshold, we could expect more “well-constrained” cases. But for a given threshold, we still find the number of well-constrained cases increases with the emission budgets.”

A few technical points:

-L35: "more than 10 times within one year" is a low number. As stated above, if this is the case, is using 20% as the only threshold discussed in the paper a reasonable choice?

**Response:**

See our discussion above about the choice of N20 as the main diagnostic to characterize the frequency of “well constrained” inversions.

-L58-59: other studies worth mentioning, for instance:

Kort, E. A., Frankenberg, C., Miller, C. E. and Oda, T.: Space-based observations of megacity carbon dioxide, *Geophys. Res. Lett.*, 39(17), n/a-n/a, doi:10.1029/2012GL052738, 2012.

Nassar, R., Hill, T. G., McLinden, C. A., Wunch, D., Jones, D. B. A. and Crisp, D.: Quantifying CO<sub>2</sub> Emissions From Individual Power Plants From Space, *Geophys. Res. Lett.*, 44(19), 10,045-10,053, doi:10.1002/2017GL074702, 2017.

Schwandner, F. M., Gunson, M. R., Miller, C. E., Carn, S. A., Eldering, A., Krings, T., Verhulst, K. R., Schimel, D. S., Nguyen, H. M., Crisp, D., O’Dell, C. W., Osterman, G. B., Iraci, L. T. and Podolske, J. R.: Spaceborne detection of localized carbon dioxide sources., *Science*, 358(6360), eaam5782, doi:10.1126/science.aam5782, 2017.

**Response:**

Thanks for the reviewer to remind some more references. In the revised introduction, we rewrite the paragraph:

Ln 55 “... Alternatively, vertically integrated columns of dry-air mole fractions of CO<sub>2</sub> (XCO<sub>2</sub>) from satellites offer the opportunity to sample the atmosphere with a global coverage. Kort et al. (2012) and Janardanan (2016) found that significant XCO<sub>2</sub> enhancements could be detected over some megacities using Greenhouse Gases Observing Satellite (GOSAT) XCO<sub>2</sub> observations. Schwandner et al. (2017) also found XCO<sub>2</sub> enhancements of 4.4 to 6.1 ppm in the Los Angeles urban CO<sub>2</sub> dome using observations from Orbiting Carbon Observatory-2 (OCO-2). Nassar et al. (2017) used the XCO<sub>2</sub> observations from OCO-2 to quantify CO<sub>2</sub> emissions from several middle- to large-sized coal power plants. However, the design of GOSAT and OCO-2 observations with sparse sampling was focused on the monitoring of CO<sub>2</sub> natural fluxes. Recent studies show a limited amount of clear detections of transects of XCO<sub>2</sub> plumes from cities or plants in OCO-2 observations (Zheng et al., 2020a) so that GOSAT and OCO-2 data keep on being hardly used to estimate CO<sub>2</sub> city emissions. The potential for reducing uncertainties in fossil fuel CO<sub>2</sub> emissions at the scale of point sources (Bovensmann et al., 2010), cities (Broquet et al., 2018; Pillai et al., 2016) and agglomerations of several cities (O’Brien et al., 2016) should dramatically change with the planned satellite missions with

imaging capabilities. These studies consistently showed that .....

-L102: "for the first time" - It is important to talk about the bright side, however, it is equally important to define the underlying assumptions clearly. The discussion came later, but I believe a higher level of clarification here will be helpful.

**Response:**

We revise the sentences Ln 101-105: “Therefore, in this study, we develop a Plume Monitoring Inversion Framework (PMIF) and conduct a set of Observing System Simulation Experiments (OSSEs) to assess, for the first time, the performance of a satellite instrument to monitor the emissions of all the clumps across the globe and over a whole year. The imager studied has the foreseen characteristics of the individual satellites of the forthcoming CO2M mission. It would be a high-resolution spectrometer, with 2 km × 2 km resolution pixels and a swath of 300 km, and it would be placed on a sun-synchronous orbit ensuring global coverage in 4 days. The PMIF inversion system relies on the list of clumps extracted by Wang et al. (2019) from the ODIAC inventory, on the Gaussian plume model to simulate the XCO<sub>2</sub> plumes generated by the emissions from these clumps, on an analytical inverse modeling framework, and on a combination of overlapping assimilation windows to solve for the inversion problem over the globe and a full year. It also addresses the question of temporal extrapolation that is needed to generate estimates of annual emissions from the information of a limited number of time windows for which emissions are well constrained by the direct satellite images, by accounting for the temporal auto-correlation of the prior uncertainties. The performance is assessed in terms of the uncertainties in the emissions (Sect. 2.1) at different scales. The PMIF uses a Gaussian plume model at the local scale to ensure that the computation cost is affordable. Such a model can often hardly fit with actual plumes over the distances considered in this study (due to variations in the wind field, topography, vertical mixing etc. over such distances) but is shown, when driven with suitable parameters, to provide a satisfactory simulation of the plume extent and amplitudes, which appear to be the main drivers of the targeted computations of uncertainties in the emissions in our OSSE framework (as shown in section 3.1). In PMIF, we also ignore the impact of some sources of uncertainties on the inversion of emissions, including systematic errors on the XCO<sub>2</sub> retrievals, the impact of uncertainties in diffuse anthropogenic emissions outside clumps, in natural CO<sub>2</sub> fluxes (within and outside clumps), and in the spatial and temporal variations of emissions within the clump and the short time windows that the inversion aims to solve. These impacts are discussed in detail afterwards.”

-L105: How about observations near the edge of the swath? The resolution would change accordingly.

**Response:**

The observations are simulated using the method and model described by Buchwitz et al. (2013) in the frame of different ESA projects studying XCO<sub>2</sub> imagers with inputs from ESA. Different values for the parameters in the model are used to account for the differences between the original configuration for CarbonSat and the configuration for CO2M.

The edge effect is small because the swath width we discussed is only 300 km. For a satellite at 700 km altitude and with a ground pixel at nadir at the resolution of 2 km, the resolution of a pixel at the edge of the swath is about 2.09 km, which is still very close to 2 km.

In fact, the edge effect is very small and very well within the overall uncertainty of the method which is based on various input data sets.

-L137:  $y_{\text{fixed}}$  is not explained.

**Response:**

We revised the sentence:

“... The inversion derives a statistical estimate for a set of control variables  $\mathbf{x}$  in a model  $\mathbf{x} \rightarrow \mathbf{y} = \mathbf{M}\mathbf{x}$  that simulates the satellite XCO<sub>2</sub> measurements  $\mathbf{y}^o$ . The model  $\mathbf{M}$  linking  $\mathbf{x}$  and  $\mathbf{y}$  is a combination of flux and atmospheric transport models (detailed in Sect. 2.4), and is called observation operator hereafter. As explained below, we do not have a constant term added to  $\mathbf{M}\mathbf{x}$  in the observation operator of the PMIF that would gather the atmospheric CO<sub>2</sub> signature of the fluxes not controlled by the inversion (like non-fossil fluxes and the background XCO<sub>2</sub> field) since the uncertainty in such fluxes is ignored. The inversion follows a Bayesian statistical framework, ...”

-L144, 148: "In this study" is used quite a lot. Not all necessary.

**Response:**

We have gone through the manuscript carefully, and removed some of them.

-L152: not accounting for diffuse CO<sub>2</sub> fluxes is an important distinction. It is an important assumption that needs to be emphasized as the natural carbon cycle will have a strong imprint in many areas.

**Response:**

We revise the sentence:

“...Therefore, we first compare the results for Paris from PMIF against those acquired based on a 3-D Eulerian atmospheric transport model by Broquet et al. (2018), the latter also accounting for uncertainties in diffuse and natural CO<sub>2</sub> fluxes. On the one hand, the signals from these diffuse and natural CO<sub>2</sub> fluxes cannot be modelled effectively by a Gaussian plume model. On the other hand, the diffuse and natural CO<sub>2</sub> fluxes in Paris was shown to have only a weak impact on the inversion of fossil fuel CO<sub>2</sub> emissions (Stauffer et al., 2016). For this comparison, ...”

In addition, we add more discussions on the impact of biogenic fluxes in more detail:

Ln 519-523: “...Broquet et al. (2018) showed that systematic error could hamper the ability of the inversion system to reduce the errors in the emissions estimates. Thirdly, we neglect the impact of uncertainties in diffuse fossil fuel CO<sub>2</sub> emissions (outside clumps) and non-fossil CO<sub>2</sub> fluxes (within and outside clumps), the latter including net ecosystem exchange (NEE) from the terrestrial biosphere, the CO<sub>2</sub> emitted by the burning of biofuel, the respiration from human and animals (Ciais et al., 2020) and the net CO<sub>2</sub> fluxes between the atmosphere and ocean. For example, the signals from terrestrial NEE can be strong during the growing season, and the signals from ocean CO<sub>2</sub> fluxes may have a critical impact on the overall XCO<sub>2</sub> patterns in the proximity of coastlines. In principle, the signals of diffuse fossil fuel CO<sub>2</sub> emissions and non-fossil CO<sub>2</sub> fluxes outside the clumps can be potentially filtered by removing the local background XCO<sub>2</sub> field to extract plumes generated only by emissions from clumps (Kuhlmann et al., 2019; Reuter et al., 2019; Ye et al., 2020; Zheng et al., 2020a). The non-fossil

CO<sub>2</sub> fluxes within clumps vary from clump to clump, and could contribute a non-negligible fraction of the total CO<sub>2</sub> fluxes in many clumps (Brón et al., 2015; Ciaï et al., 2020; Wu et al., 2018). The satellite observations alone cannot effectively differentiate the fossil fuel CO<sub>2</sub> emissions and the non-fossil CO<sub>2</sub> fluxes within clumps. In the clumps with non-negligible non-fossil CO<sub>2</sub> fluxes, the inversion of fossil fuel CO<sub>2</sub> emissions could be influenced (Ye et al., 2020; Yin et al., 2019). Fourthly, ...”

-L225: a simple description of the sigma parameter (e.g., what determines it) will help the reader without having to refer to Ars et al. (2017).

**Response:**

To clarify our set-up of the parameters in the Gaussian plume model used here, we revise the sentence in Ln 225: “The  $\sigma_j$  is a function of downwind distance  $i$  and atmospheric stability parameter:  $\sigma_j = \beta j / (1 + \gamma j)^{-1/2}$ , where  $\alpha$  is a coefficient that converts the computed XCO<sub>2</sub> enhancement in the unit of ppm, and  $\beta$  and  $\gamma$  are coefficients depending on the atmospheric Pasquill stability category which is a function of the wind speed and solar radiation (Turner, 1970). The values for  $\beta$  and  $\gamma$  can be found in Bowers et al. (1980). The original Gaussian plume model generates a stationary plume... ”

-L369: why not just use Fig. S3 for side by side comparison?

**Response:**

Fig. S3b is adapted from from Fig. 6 in Broquet et al. (2018), Copernicus Publications. We assume it is not allowed to put it in the main text. If the editor can confirm it can be put in the main text without any copyright issue, we agree to replace Fig. 1 with Fig. S3.

-L404: "N20". There are quite some acronyms already that need checking back and forth. Will improve the reading removing some that do not have intuitive meanings.

**Response:**

We have acronyms of “N20”, “D20” for the assessment of the posterior uncertainties. We also have acronyms of “AMS”, “ASS”, “MCS”, “SCS”, “SectCS”, “NoCor” for the configuration of prior uncertainty. Each acronym has a long explanation, and we found it is not easy to adapt the manuscript without using these acronyms. However, we summarize all the acronyms in an Appendix to help the readers.

-L501: How about the optimized state? Curious how well will the Gaussian Plum model do if it assimilates the psuedo observations generated using the full 3-D models in this case. It will be a strong demonstration if it can get the emission order general variations right!

**Response:**

As it stands, PMIF can be used to process individual samples of pseudo prior fluxes and pseudo observations and compute pseudo posterior fluxes to assess error reductions to a pseudo truth. All the numerical objects needed to apply Eq.2 are built in this system as reflected by its description. However, if the errors injected in such OSSEs with explicit pseudo data are consistent with the statistics of uncertainties know by the inversion system, the statistics of errors in the flux estimates are fully characterized by  $\mathbf{A}$  (since the observation operator is linear), whose direct computation is thus the best index of the potential of the inversion and of a given

observation network (Wang et al., 2018). This is why we only focus on such a computation here.

PMIF is mainly designed for OSSEs and would require some adaptations and extensions to process real satellite images or the pseudo observations generated by a 3-D model. For example, it requires to remove the XCO<sub>2</sub> background concentrations underlying the detected plumes in the observations that could be assimilated by the system. More importantly, the Gaussian model may have difficulties to fit the plumes generated by a 3-D model in some cases: because of the turbulence close to the source, of the 3D variations in the wind field, and of multiple other parameters (like variations in the topography, the complexity of vertical mixing etc.). As done by Nassar et al. (2017), the wind direction might need some adjustment in some cases.

However, the difficulty of fitting the model simulation to the actual plumes sampled by the observation is also a traditional weakness in atmospheric inversion when the complex mesoscale atmospheric transport models are used; this explains why many of the recent inversions of CO<sub>2</sub>/CH<sub>4</sub> plant and city emissions that have been conducted based on OCO-2/TROPOMI data use Gaussian models or a Gaussian approximation of the shape of the plume to apply direct flux computations in the data (e.g. Nassar et al., 2017; Reuter et al., 2019; Zheng et al., 2020).

In addition, the study by Prunet et al. (2020) (the talk available at [https://cdn.eventsforce.net/files/ef-xnn67yq56yly/website/9/5\\_734\\_pascal\\_prunet-plume\\_detection\\_and\\_characterization\\_from\\_xco\\_imagery-evaluation\\_of\\_gaussian\\_methods\\_for\\_quantifying\\_plant\\_and\\_city\\_fluxes.pptx](https://cdn.eventsforce.net/files/ef-xnn67yq56yly/website/9/5_734_pascal_prunet-plume_detection_and_characterization_from_xco_imagery-evaluation_of_gaussian_methods_for_quantifying_plant_and_city_fluxes.pptx)) indicates that Gaussian models fit the plumes from true mesoscale models well enough (so that the inversions using the Gaussian model can provide a good estimate of the emissions) for a good part of the typical atmospheric conditions encountered around the set of European cities and plants they investigated.

So we think the use of a Gaussian plume model does not bias the results discussed in the paper given the considerations listed above.

-L519: Quite a few studies explore the interfering effect of natural CO<sub>2</sub> fluxes.

Wu, K., Lauvaux, T., Davis, K. J., Deng, A., Lopez Coto, I., Gurney, K. R. and Patarasuk, R.: Joint inverse estimation of fossil fuel and biogenic CO<sub>2</sub> fluxes in an urban environment: An observing system simulation experiment to assess the impact of multiple uncertainties, *Elem Sci Anth*, 6(1), 17, doi:10.1525/elementa.138, 2018.

Yin, Y., Bowman, K., Bloom, A., Worden, J.: Detection of fossil fuel emission trends in the presence of natural carbon cycle variability, *Environmental Research Letter*, 14(8):084050, doi:10.1088/1748-9326/ab2dd7, 2019.

**Response:**

See the response before about non-fossil CO<sub>2</sub> fluxes.

-L538: Again, I understand that 20% posterior uncertainty is a desirable goal, but it did not provide a full picture if the values for the high emission densities are only at the order of 10 days for a year. Other references will help define the landscape.

**Response:**

As discussed above, this 20% threshold is used to quantify only the cases when the emissions are “well constrained”.

In this paragraph, what we want to discuss is the large variation of N20 within each emission bin. If we choose other threshold, it does not change the fact that the clumps within each bin are not be equally constrained: the frequency of clear-sky days still largely impacted the performance of the inversion.

-Figure 3: the number of clumps is repeated in every plot from Fig. 3-5. Reductant to repeat so many times. Maybe indicate clearly that (a) and (b) are the same just for different experiments.

**Response:**

We remove the number of clumps in Figs. 3-5.

**References**

Bowers, J. F., Bjorklund, J. R., Cheney, C. S. and Schewe, G. J.: Industrial source complex (ISC) dispersion model user’s guide, US Environmental Protection Agency, Office of Air Quality Planning and Standards., 1980.

Bréon, F. M., Broquet, G., Puygrenier, V., Chevallier, F., Xueref-Remy, I., Ramonet, M., Dieudonné, E., Lopez, M., Schmidt, M., Perrussel, O. and Ciais, P.: An attempt at estimating Paris area CO<sub>2</sub> emissions from atmospheric concentration measurements, *Atmospheric Chemistry and Physics*, 15(4), 1707–1724, doi:10.5194/acp-15-1707-2015, 2015.

Ciais, P., Wang, Y., Andrew, R., Bréon, F.-M., Chevallier, F., Broquet, G., Nabuurs, G.-J., Peters, G., McGrath, M., Meng, W., Zheng, B. and Tao, S.: Biofuel burning and human respiration bias on satellite estimates of fossil fuel CO<sub>2</sub> emissions, *Environ. Res. Lett.*, doi:10.1088/1748-9326/ab7835, 2020.

Janardanan, R., Maksyutov, S., Oda, T., Saito, M., Kaiser, J. W., Ganshin, A., Stohl, A., Matsunaga, T., Yoshida, Y. and Yokota, T.: Comparing GOSAT observations of localized CO<sub>2</sub> enhancements by large emitters with inventory-based estimates, *Geophys. Res. Lett.*, 43(7), 2016GL067843, doi:10.1002/2016GL067843, 2016.

Kort, E. A., Frankenberg, C., Miller, C. E. and Oda, T.: Space-based observations of megacity carbon dioxide, *Geophys. Res. Lett.*, 39(17), L17806, doi:10.1029/2012GL052738, 2012.

Kuhlmann, G., Broquet, G., Marshall, J., Clément, V., Löscher, A., Meijer, Y. and Brunner, D.: Detectability of CO<sub>2</sub> emission plumes of cities and power plants with the Copernicus Anthropogenic CO<sub>2</sub> Monitoring (CO<sub>2</sub>M) mission, *Atmospheric Measurement Techniques Discussions*, 1–35, doi:https://doi.org/10.5194/amt-2019-180, 2019.

Nassar, R., Hill, T. G., McLinden, C. A., Wunch, D., Jones, D. B. A. and Crisp, D.: Quantifying CO<sub>2</sub> Emissions From Individual Power Plants From Space, *Geophys. Res. Lett.*, 44, 10045–10053, doi:10.1002/2017GL074702, 2017.

Reuter, M., Buchwitz, M., Schneising, O., Krautwurst, S., O’Dell, C. W., Richter, A.,

Bovensmann, H. and Burrows, J. P.: Towards monitoring localized CO<sub>2</sub> emissions from space: co-located regional CO<sub>2</sub> and NO<sub>2</sub> enhancements observed by the OCO-2 and S5P satellites, *Atmospheric Chemistry and Physics*, 19(14), 9371–9383, doi:<https://doi.org/10.5194/acp-19-9371-2019>, 2019.

Schwandner, F. M., Gunson, M. R., Miller, C. E., Carn, S. A., Eldering, A., Krings, T., Verhulst, K. R., Schimel, D. S., Nguyen, H. M., Crisp, D., O'Dell, C. W., Osterman, G. B., Iraci, L. T. and Podolske, J. R.: Spaceborne detection of localized carbon dioxide sources, *Science*, 358(6360), eaam5782, doi:10.1126/science.aam5782, 2017.

Staufer, J., Broquet, G., Bréon, F.-M., Puygrenier, V., Chevallier, F., Xueref-Rémy, I., Dieudonné, E., Lopez, M., Schmidt, M., Ramonet, M., Perrussel, O., Lac, C., Wu, L. and Ciais, P.: The first 1-year-long estimate of the Paris region fossil fuel CO<sub>2</sub> emissions based on atmospheric inversion, *Atmos. Chem. Phys.*, 16(22), 14703–14726, doi:10.5194/acp-16-14703-2016, 2016.

Turner, D. B.: Workbook Of Atmospheric Dispersion Estimateates. Office of Air Program Pub. No. AP-26, Environmental protection agency, USA., 1970.

Wang, Y., Broquet, G., Ciais, P., Chevallier, F., Vogel, F., Wu, L., Yin, Y., Wang, R. and Tao, S.: Potential of European 14CO<sub>2</sub> observation network to estimate the fossil fuel CO<sub>2</sub> emissions via atmospheric inversions, *Atmos. Chem. Phys.*, 18(6), 4229–4250, doi:10.5194/acp-18-4229-2018, 2018.

Wu, K., Lauvaux, T., Davis, K. J., Deng, A., Coto, I. L., Gurney, K. R. and Patarasuk, R.: Joint inverse estimation of fossil fuel and biogenic CO<sub>2</sub> fluxes in an urban environment: An observing system simulation experiment to assess the impact of multiple uncertainties, *Elem Sci Anth*, 6(1), 17, doi:10.1525/elementa.138, 2018.

Ye, X., Lauvaux, T., Kort, E. A., Oda, T., Feng, S., Lin, J. C., Yang, E. G. and Wu, D.: Constraining Fossil Fuel CO<sub>2</sub> Emissions From Urban Area Using OCO-2 Observations of Total Column CO<sub>2</sub>, *Journal of Geophysical Research: Atmospheres*, 125(8), e2019JD030528, doi:10.1029/2019JD030528, 2020.

Yin, Y., Bowman, K., Bloom, A. A. and Worden, J.: Detection of fossil fuel emission trends in the presence of natural carbon cycle variability, *Environ. Res. Lett.*, 14(8), 084050, doi:10.1088/1748-9326/ab2dd7, 2019.

Zheng, B., Chevallier, F., Ciais, P., Broquet, G., Wang, Y., Lian, J. and Zhao, Y.: Observing carbon dioxide emissions over China's cities and industrial areas with the Orbiting Carbon Observatory-2, *Atmospheric Chemistry and Physics*, 20(14), 8501–8510, doi:<https://doi.org/10.5194/acp-20-8501-2020>, 2020a.

Zheng, B., Chevallier, F., Ciais, P., Broquet, G., Wang, Y., Lian, J. and Zhao, Y.: Observing carbon dioxide emissions over China's cities with the Orbiting Carbon Observatory-2, *Atmospheric Chemistry and Physics Discussions*, 1–17, doi:<https://doi.org/10.5194/acp-2020->

123, 2020b.